Molecular Beam Studies of Elementary Chemical Processes

YUAN TSEH LEE

CHEMISTRY IS THE STUDY OF MATERIAL TRANSFORMATIONS. Yet a knowledge of the rate, or time dependence, of chemical change is of critical importance for the successful synthesis of new materials and for the utilization of the energy generated by a reaction. During the past century it has become clear that all macroscopic chemical processes consist of many elementary chemical reactions that are themselves simply a series of encounters between atomic or molecular species. To understand the time dependence of chemical reactions, chemical kineticists have traditionally focused on sorting out all of the elementary chemical reactions involved in a macroscopic chemical process and determining their respective rates.

Our basic understanding of the relation between reactive molecular encounters and rates of reactions [formulated in terms of activation energies, E_a, and preexponential factors, A, as elucidated by Arrhenius in his rate constant expression, $k = A \exp(-E_a/RT)$ where k is the rate constant, R is the gas constant, and T is the temperature] was deepened some 50 years ago following the discovery of quantum mechanics. Since a chemical reaction is fundamentally a mechanical event, involving the rearrangement of atoms and molecules during a collision, detailed information on the dynamics of simple chemical reactions could be obtained by first carrying out extensive quantum mechanical calculations of the interaction potential as a function of interatomic distances and then computing classical trajectories based on this potential energy surface (*1*). Although these initial theoretical studies were only qualitative, they heralded a new era in the field of chemical kinetics; the chemist could now, in principle, predict the dynamical course of a chemical reaction.

During the past three decades, with the development of many sophisticated experimental techniques, it has become possible to study the dynamics of elementary chemical reactions in the laboratory. For example, detailed information on the nascent quantum state distributions of simple products for some chemical reactions can be derived from the chemiluminescence spectra of reaction products obtained under single collision conditions (*2*), the analysis of the threshold operating conditions of a chemical laser (*3*), or the spectra obtained with the use of various linear or nonlinear laser spectroscopic techniques (*4, 5*). However, when one desires to (i) control the energies of the reagents, (ii) understand the dependence of chemical reactivity on molecular orientation, (iii) explore the nature of reaction intermediates and their subsequent decay dynamics, and (iv) identify complex reaction mechanisms involving polyatomic radical products, the crossed–molecular beam technique is most suitable (*6, 7*).

Information derived from the measurements of angular and velocity distributions of reaction products played a crucial role in the advancement of our understanding of the dynamics of elementary chemical reactions. This and the more general investigations of chemical reactions under single collision conditions in crossed molecular beams will be the subject of this lecture.

Crossed–Molecular Beam Experiments: Product Distribution Measurements

If the motion of individual atoms were observable during reactive collisions between molecules, it would be possible to understand exactly how a chemical reaction takes place by just following the motion of these atoms. Unfortunately, despite recent advances in microscope technology that allow us to observe the static arrangement of atoms in a solid, we are still far from being able to follow the motion of atoms in the gas phase in real time. Crossed–molecular beam experiments make it possible to "visualize" the details of a chemical reaction by tracing the trajectories of the reaction products. This is done by first defining the velocities, approach angle, and other initial conditions of the reactants, and then measuring the velocity and angular distributions of the products. For example, in the investigation of the reaction $F + D_2 \rightarrow DF + D$ (*8*), if we let fluorine atoms and D_2 molecules collide at a relative energy of 1.82 kcal/mol and then measure the angular and velocity distributions of DF products, we will obtain the results shown in Fig. 1. This contour map shows the probability of DF products appearing at specific angles and velocities and reveals a great deal about the dynamics of the reaction. The initial direction of the fluorine atom beam is 0°, and the distance between any point and the center is the center-of-mass velocity. The strong backward peaking of DF products with respect to the initial direction of fluorine atoms indicates that not all the collisions between fluorine atoms and D_2 molecules produce DF product. Only those collisions in which the fluorine atom and the two deuterium atoms are nearly linear will lead to a reaction and produce DF. Apparently, if a fluorine atom collides with a D_2 molecule from a direction perpendicular to the molecular axis of the D_2, the fluorine atom will only bounce off elastically. The appearance of DF in several velocity bands is due to the fact that DF molecules are produced in several vibrational states with different recoil velocities as indicated in Fig. 1. Since the total energy released in every reactive encounter between fluorine and D_2 is the same, the maximum energy available for translational motion will depend on the vibrational quantum state of DF. Because the rotational energy spread of DF products is less than the spacings of the vibrational energy levels, the recoil velocities of various vibrational states of DF products are well separated and can be identified easily.

If a crossed–molecular beam study of this reaction is carried out

---

The author is professor of chemistry at the University of California, Berkeley, CA 94720. This article is a condensed version of the lecture he delivered in Stockholm, Sweden, 8 December 1986, when he received the Nobel Prize in Chemistry, which he shared with John C. Polanyi and Dudley R. Herschbach. It is published here with the permission of the Nobel Foundation and will also be included in the complete volume of *Les Prix Nobel en 1986* as well as in the series *Nobel Lectures* (in English) published by Elsevier Publishing Company, Amsterdam and New York. Dr. Polanyi's lecture appeared in the 8 May issue and that of Dr. Herschbach will be in a subsequent issue.

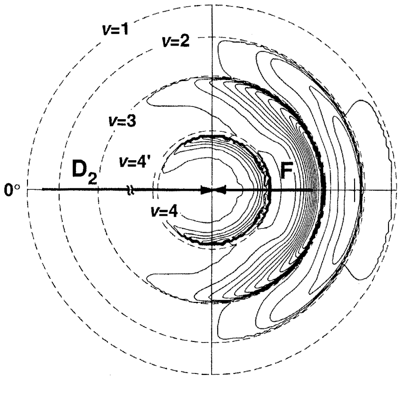

Fig. 1. Center-of-mass velocity flux contour map for the F + $D_2 \rightarrow$ DF + D reaction. Fluorine atoms and D_2 molecules move toward each other at a collision energy of 1.82 kcal/mol, with the fluorine atoms moving from right to left.

with the experimental arrangement shown in Fig. 2, the rate of production of DF products, dN_{DF}/dt, in the scattering volume defined by the crossing of two beams can be estimated from the following equation:

$$\frac{dN_{DF}}{dt} = n_F n_{D_2} \sigma g \Delta V$$

where n_F and n_{D_2} are the number densities of fluorine atoms and D_2 molecules in the scattering region, and σ, g, and ΔV are the reaction cross section, the relative velocity between F and D_2, and the scattering volume, respectively. In an experiment with a velocity-selected effusive fluorine atom source and a supersonic beam of D_2, the values of n_F, n_{D_2}, and ΔV are typically 10^{10} molecules per cubic centimeter, 10^{12} molecules per cubic centimeter, and 10^{-2} cm^3. If the relative velocity between fluorine and D_2 is 10^5 cm/sec and the reactive cross section is 10^{-15} cm^2, then dN_{DF}/dt will have a value of 10^{10} molecules per second. These DF products with various recoil velocities will scatter into a range of laboratory angles. If the DF is scattered fairly evenly within 1 steradian of solid angle in the laboratory and if the movable detector which scans the angular distribution has an acceptance solid angle of 1/3000 steradian (approximately an angular width of 1° in both directions from the detector axis), the detector will receive $\sim 3 \times 10^6$ DF molecules per second.

To detect the DF products, however, first it is necessary to ionize DF to DF^+ by electron bombardment. The product ion can then be mass filtered and counted. The typical ionization efficiency for a molecule during the short transit time through the ionizer is about 10^{-4}. A DF flux of 3×10^6 molecules per second reaching the detector will yield only 300 DF^+ ions per second. However, this is a large enough number to allow reliable measurements of angular and velocity distributions in a relatively short time if the background count rate is not much greater. Indeed, the success of a crossed–molecular beam study of such a chemical reaction depends entirely on whether the background in the mass spectrometric detector can be reduced sufficiently (*9*).

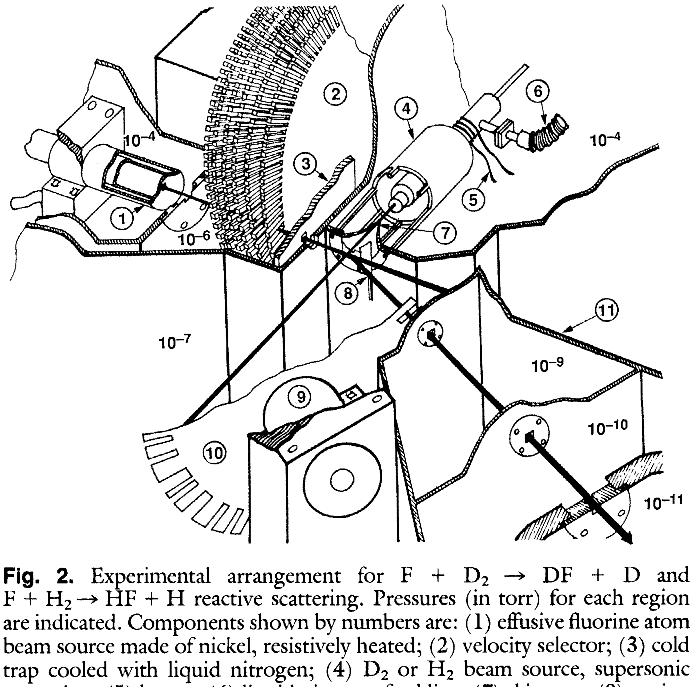

Fig. 2. Experimental arrangement for F + $D_2 \rightarrow$ DF + D and F + $H_2 \rightarrow$ HF + H reactive scattering. Pressures (in torr) for each region are indicated. Components shown by numbers are: (1) effusive fluorine atom beam source made of nickel, resistively heated; (2) velocity selector; (3) cold trap cooled with liquid nitrogen; (4) D_2 or H_2 beam source, supersonic expansion; (5) heater; (6) liquid nitrogen feed line; (7) skimmer; (8) tuning fork chopper; (9) synchronous motor; (10) cross-correlation chopper for time-of-flight velocity analysis; and (11) ultrahigh vacuum, triply differentially pumped, mass spectrometric detector chamber.

There are two sources of background molecules in the detector used in a crossed–molecular beam experiment: the inherent background in the detector chamber and the background caused by the effusion of molecules from the collision chamber into the detector when the beams are on. The former is due mainly to outgassing from the materials used for the construction of the chamber and to limitations imposed by the performance of the ultrahigh vacuum pumping equipment. Reduction of the latter requires many stages of differential pumping with buffer chambers (*10*).

Direct Experimental Probing of Potential Energy Surfaces

For gaseous rare gas systems, if the interaction potentials between the atoms are accurately known, all bulk properties and transport phenomena can be predicted theoretically. Similarly, for a simple atom-molecule reaction, the potential energy surface, which describes the interaction potential as a function of the coordinates of the atoms, will be the basis for understanding the detailed dynamics of a chemical reaction.

One of the systems that has attracted extensive attention in both experimental and theoretical efforts during the last 15 years is the reaction F + $H_2 \rightarrow$ HF + H. In the early 1970s, using quasiclassical trajectory calculations, Muckerman derived a semiempirical potential energy surface, known as the Muckerman V surface, that gave results in agreement with all experimental data available at that time (*11*). These results included rate constants, vibrational-rotational state distributions obtained from chemical laser and chemiluminescence experiments, as well as product angular distributions obtained from F + $D_2 \rightarrow$ DF + D experiments as shown in Fig. 1. The potential energy surface obtained from the ab initio quantum mechanical calculations (*12*) was still rather limited at that time, but it did show many important features that were in good qualitative agreement with the Muckerman V surface.

If the Muckerman V surface were sufficiently accurate, it would be possible to carry out scattering calculations with this surface under conditions that could not be easily arranged in the laboratory. This would significantly expand the scope of our understanding of the dynamics of this system. However, the accuracy of the Muckerman V surface depends not only on the reliability of the experimental input used in the derivation of the surface, but also on the applicability of classical mechanics in treating the F + $H_2 \rightarrow$ HF + H reaction. This is certainly a major concern for a hydrogen atom transfer reaction.

One-dimensional quantum calculations on the F + H_2 reaction, although not necessarily realistic, had in fact shown the inadequacy of classical mechanics in handling this reaction (*13, 14*). Quantum effects were, indeed, very important, and in all these calculations strong "resonances" were found in the dependence of reaction

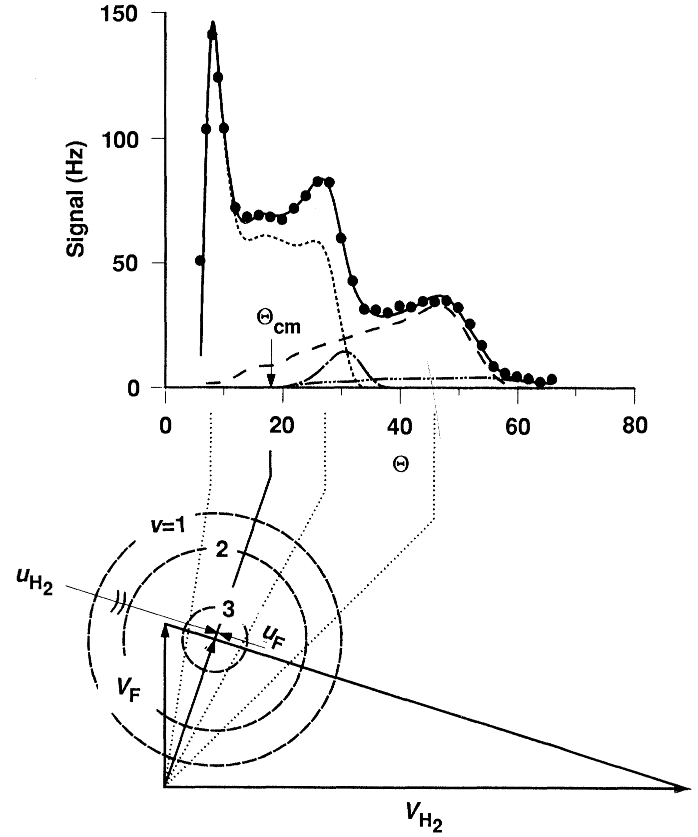

Fig. 3. Laboratory angular distribution for F + *para*-H_2 for a collision energy of 1.84 kcal/mol. The velocity diagram is shown below. Both the data (**top**) and calculated laboratory distributions are shown. (●) Data, (——) total calculated distribution, (— · · · —) $v = 1$ component, (– – –) $v = 2$ component, (- - - -) $v = 3$ component, (— · —) $v = 3'$ component [from $H_2(J = 2)$]. u_{H_2}, u_F, V_{H_2}, and V_F (**bottom**) are velocity vectors for H_2 and F in the center of mass and in the laboratory frame, respectively. Θ_{cm} denotes the direction of the velocity vector of the center of mass of the entire system measured from V_F.

probability on collision energy (*15*). These resonances were later shown to be due to the formation of "quasi-bound" states in the F–H–H reaction intermediate (*16, 17*). The F + H_2 surface has a barrier in the entrance channel, but there is no attractive well in the intimate region near the transition state. The quasi-bound states in the F + H_2 reaction are entirely dynamical in nature. Loosely speaking, the first dynamic resonance is due to the formation of a bound state which is a superposition of F + $H_2(v = 0)$ and $HF(v = 3)$ + H where v in the vibrational level, in the intimate region of chemical interaction.

The discovery of dynamical resonances in the collinear quantum calculations of the F + H_2 system provided new possibilities for probing the critical region of the potential energy surface more directly. In contrast to most other microscopic experiments, in which the influence of the potential energy surface on the final distribution of products is assessed, the experimental observation of resonances is almost equivalent to carrying out vibrational spectroscopic measurements directly on the reaction intermediate. Thus it should offer a more stringent test of the details of the calculated potential energy surface (*16*).

In a three-dimensional quantum scattering calculation of F + H_2 on the Muckerman V surface, Wyatt *et al.* (*18*) have shown that as the collision energy is increased beyond the one-dimensional resonance energy, the resonance does not just disappear but occurs at increasingly larger impact parameters. Consequently, resonances cannot be observed in an experiment in which the reaction cross section is measured as a function of collision energy. On the other hand, if the experiment is carried out at a fixed collision energy, and if the reaction probability is measured as a function of impact parameter, the resonance should be observable. Unfortunately, one has no hope of controlling or measuring the impact parameter in a scattering experiment. But, for F + $H_2 \rightarrow$ HF + H, in which the collinear configuration dominates the reactive scattering at lower collision energies, the scattering angle of HF should depend on the impact parameter. In particular, when a quasi-bound state is formed, if the average lifetime of the F–H–H intermediate is an appreciable fraction of its rotational period, HF produced from the decay of the F–H–H quasi-bound state is expected to scatter in a more forward direction; by comparison, the direct reaction produces strongly backward peaked HF. One of the unique and most important aspects of the measurement of product angular distributions is that one can use the rotational period of the reaction intermediate, typically 10^{-12} to 10^{-13} second, to judge the lifetime of the reaction intermediate (*6*). If the average lifetime of the intermediate is much longer than the rotational period, the angular distribution of products will show forward-backward symmetry. On the other hand, if the lifetime is much shorter, the asymmetric angular distribution reveals the preferred molecular orientation for the chemical reaction to occur.

Experimental measurements of the laboratory angular distribu-

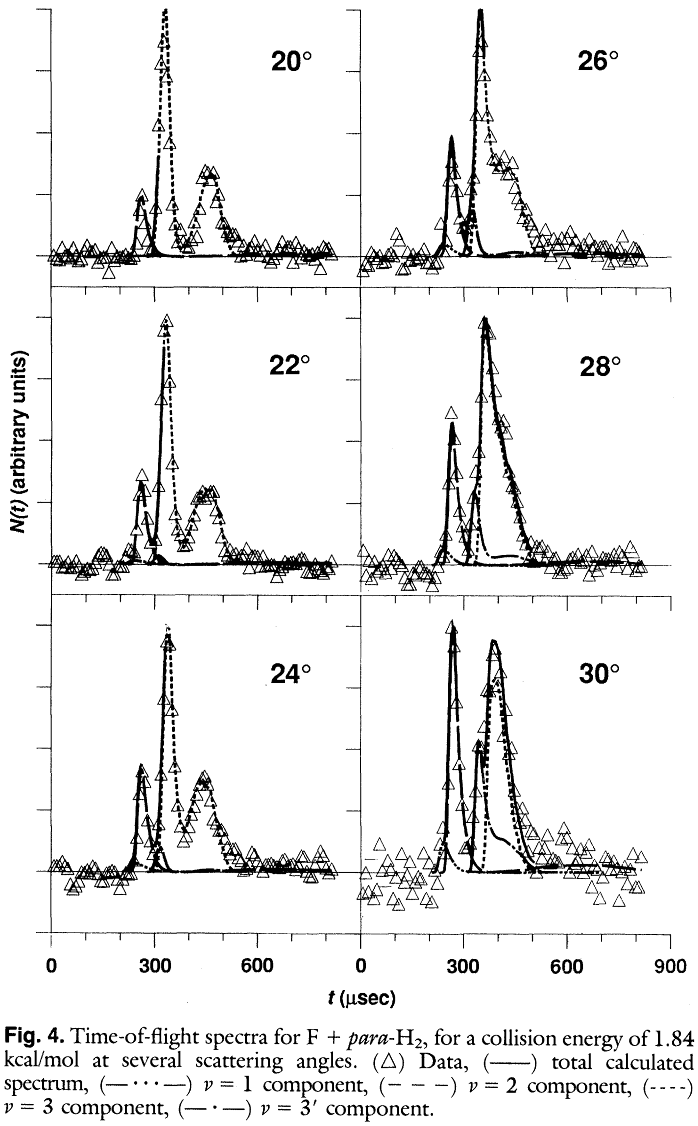

Fig. 4. Time-of-flight spectra for F + *para*-H_2, for a collision energy of 1.84 kcal/mol at several scattering angles. (△) Data, (——) total calculated spectrum, (— · · · —) $v = 1$ component, (– – –) $v = 2$ component, (- - - -) $v = 3$ component, (— · —) $v = 3'$ component.

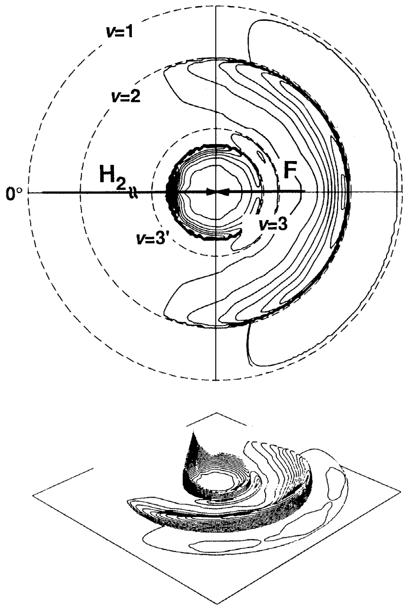

Fig. 5. (**Top**) Center-of-mass velocity flux contour map for F + *para*-H_2, with a collision energy of 1.84 kcal/mol. (**Bottom**) Contour map in three-dimensional perspective.

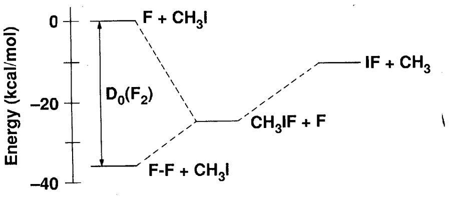

Fig. 6. Energy diagram showing the relative energy of the CH_3IF intermediate in the reaction of $F + CH_3I \rightarrow CH_3 + IF$ and as a product of the endothermic $F_2 + CH_3I \rightarrow CH_3IF + F$ reaction.

tion and time-of-flight velocity distributions of HF products at a collision energy of 1.84 kcal/mol, with the experimental arrangement shown in Fig. 2, are shown in Figs. 3 and 4. The velocity and angular distributions in the center-of-mass coordinate system derived from these experimental results are shown in Fig. 5 (*19*). The enhanced forward peaking in the angular distribution of HF in $v = 3$ is a strong indication that quasi-bound states are indeed formed in the $F + H_2 \rightarrow HF + H$ reaction at this energy, and that they seem to decay exclusively into HF in the $v = 3$ state rather than the $v = 2$ state.

This disagreement is certainly due to the shortcoming in the Muckerman V surface. These vibrationally state-specific angular distributions obtained at various collision energies for F + H_2, HD, and D_2 reactions provide a stringent test for the ever improving potential energy surfaces obtained from ab initio quantum mechanical calculations.

Exploration of New Chemistry Under Single Collision Conditions

There are many mysterious phenomena in nature that have thus far defied explanations. The mystery is often due to the fact that a certain phenomenon cannot be understood on the basis of our established knowledge or common sense.

The ease with which F_2 and I_2 react to produce electronically excited IF molecules that relax through photon emission was a mystery a dozen years ago (*20*). A molecule-molecule reaction is supposed to have a high energy barrier and the four-center reaction producing two IF molecules, with either both in the ground state or one of them in an excited state, is a symmetry-forbidden process. The textbook mechanism has either I_2 or F_2 molecules first dissociating into atoms followed by the radical chain reactions $F + I_2 \rightarrow IF + I$ and $I + F_2 \rightarrow IF + F$. However, neither of these reactions is exothermic enough to produce electronically excited IF.

The clue that something new might be happening in this reaction was actually discovered in a crossed–molecular beam study of the $F + CH_3I \rightarrow IF + CH_3$ reaction (*21*). When we found that this reaction proceeded through the formation of a long-lived complex, we began to increase the collision energy to see whether it was possible to shorten the lifetime enough to make it comparable to the rotational period of the CH_3IF complex. If we could estimate the lifetime of the collision complex with the rotational period as a clock, it would be possible to evaluate the stability of this reaction intermediate by means of statistical theories for the unimolecular decomposition rate constants. At higher collision energies, the angular distribution of products monitored at a mass-to-charge ratio $m/e = 146$ (IF^+) showed a peculiar feature that could not possibly arise from IF produced in the $F + CH_3I$ reaction. This was later shown to be from stable CH_3IF produced in the collision volume of the two beams which yielded additional IF^+ signal after dissociative ionization.

The stable CH_3IF was in fact formed by the reaction of undissociated F_2 in our F-atom beam with CH_3I:

$$CH_3I + F_2 \rightarrow CH_3IF + F$$

The threshold for this reaction was found to be 11 kcal/mol. Since the dissociation energy of F_2 is 37 kcal/mol, the dissociation energy of $CH_3IF \rightarrow CH_3I + F$ could be as high as 26 kcal/mol (Fig. 6). This was certainly a surprising result and was entirely unsuspected.

In the reaction of I_2 and F_2, it was not surprising that the stability of the I_2F radical is the driving force for the reaction

$$I_2 + F_2 \rightarrow I_2F + F$$

But what amazed us most was that this reaction had a threshold of only 4 kcal/mol, and that at 7 kcal/mol the reaction

$$I_2 + F_2 \rightarrow I + IF + F$$

was observed (*22*). In this reaction I and IF are probably produced through the secondary decomposition of vibrationally excited I_2F radicals. Later, a careful investigation showed that the threshold energy for producing electronically excited iodofluoride, IF* (*23*), in the reaction

$$I_2 + F_2 \rightarrow IF^* + IF$$

is identical to that for I_2F + F formation. However, the formation of electronically excited IF* is only a minor channel compared to I_2F + F formation. Apparently, it is a secondary encounter between the departing fluorine atom and the terminal iodine atom in I_2F that produces IF*. A relatively rare sequential process during a binary collision between F_2 and I_2 is responsible for the production of electronically excited IF, not the symmetry-forbidden four-center reaction which breaks and forms two bonds simultaneously.

The fact that one can control kinetic energy precisely and carry out a synthetic study of delicate new radicals through endothermic reactions is certainly among the most dramatic features of crossed–molecular beam experiments.

The development of the seeded supersonic beam source has been largely responsible for making crossed–molecular beam experiments at higher collision energies possible (*24*). If a gaseous mixture is expanded into a vacuum chamber through a small nozzle with a sufficiently high stagnation pressure, all molecules, regardless of their molecular weights, attain the same average terminal speed. Consequently, the kinetic energies of molecules in the beam will be proportional to their molecular weights, and for heavier atoms or molecules a very high kinetic energy can be obtained by seeding a small fraction of heavy particles in a very light carrier gas.

In a recent series of investigations of substantially endothermic reactions of bromine atoms with *ortho*-, *meta*-, and *para*-chlorotoluenes, a beam of energetic bromine atoms was used to study the reactivity and dynamics of chlorine atom substitution by bromine atoms (*25*). The intermediates of these reactions are expected to have potential wells that are much shallower than the endothermicity of reaction. From the measurements of the translational energy dependence of the reaction cross sections and the product translational energy distributions, the extent of energy randomization among various vibrational degrees of freedom was found to be rather limited. Despite the fact that *ortho*- and *para*-chlorotoluenes react easily, no substitution was observed for *meta*-chlorotoluene. This indicates that the electron density distribution on the benzene ring strongly influences the reactivity, even though dynamic factors are expected to be more important in endothermic substitution reactions.

Elucidation of Reaction Mechanisms from Product Angular and Velocity Distributions

In elementary chemical reactions involving complicated polyatomic molecules, the unraveling of the reaction mechanism is often the most important issue. Without the positive identification of primary products, it is not possible to discuss reaction dynamics in a meaningful way. In bulk experiments, the identification of primary products has often been complicated by fast secondary reactions of primary products. Recently, advances in sensitive detection methods and time-resolved laser techniques have allowed single collision experiments to become possible even in the bulk, and complications caused by secondary collisions can be avoided. However, the positive identification of internally excited polyatomic radicals produced under single collision conditions is still a difficult problem. Spectroscopic techniques that are so powerful in providing state-resolved detection of atoms or diatomic molecules are often not very useful, either because of the lack of spectroscopic information or simply because huge numbers of states are involved. The more general mass spectrometric technique, which depends heavily on "fingerprints" of fragment ions for positive identification, also suffers from the fact that fragmentation patterns for vibrationally excited polyatomic radical products in electron bombardment ionization are not known. This problem is especially serious because many radicals do not yield parent ions. Even if stable molecules are formed as products, the change in fragmentation patterns with increasing internal energy can be so drastic that erroneous conclusions are often reached. For example, at room temperature both ethanol (C_2H_5OH) and acetaldehyde (CH_3CHO) will yield $C_2H_5OH^+$ and CH_3CHO^+ as major ions by electron bombardment ionization. However, since both these ions contain a very weak bond and most of the vibrational energy is retained in the ionization process, when highly vibrationally excited C_2H_5OH and CH_3CHO are ionized, even if parent ions are initially produced, they will further dissociate into $C_2H_5O^+$ and CH_3CO^+ by ejecting a hydrogen atom (*26*).

The problem of product identification caused by the fragmentation of primary products during the ionization process can be overcome if product angular and velocity distributions are measured carefully in high-resolution crossed–molecular beam experiments. For example, the reaction between $O(^3P)$ and C_2H_4 under single collision conditions, with a mass spectrometer used to detect the products, yields signals at *m/e* = 43, 42, 29, 27, and 15. The fact that *m/e* = 15 (CH_3^+) and 29 (HCO^+) are the most intense signals suggests that CH_3 + HCO is the major reaction channel. This conclusion is in agreement with previous studies of the reaction of $O(^3P)$ with C_2H_4 carried out by Cvetanovic (*27*), Pruss *et al.* (*28*), and Blumenberg *et al.* (*29*). From the analysis of final products in a bulk experiment by means of photoionization detection of products with hydrogen Lyman-α (10.2 eV) radiation and electron bombardment ionization mass spectrometry, it was concluded that formation of CH_3 and HCO, resulting from 1-2 migration of a hydrogen atom

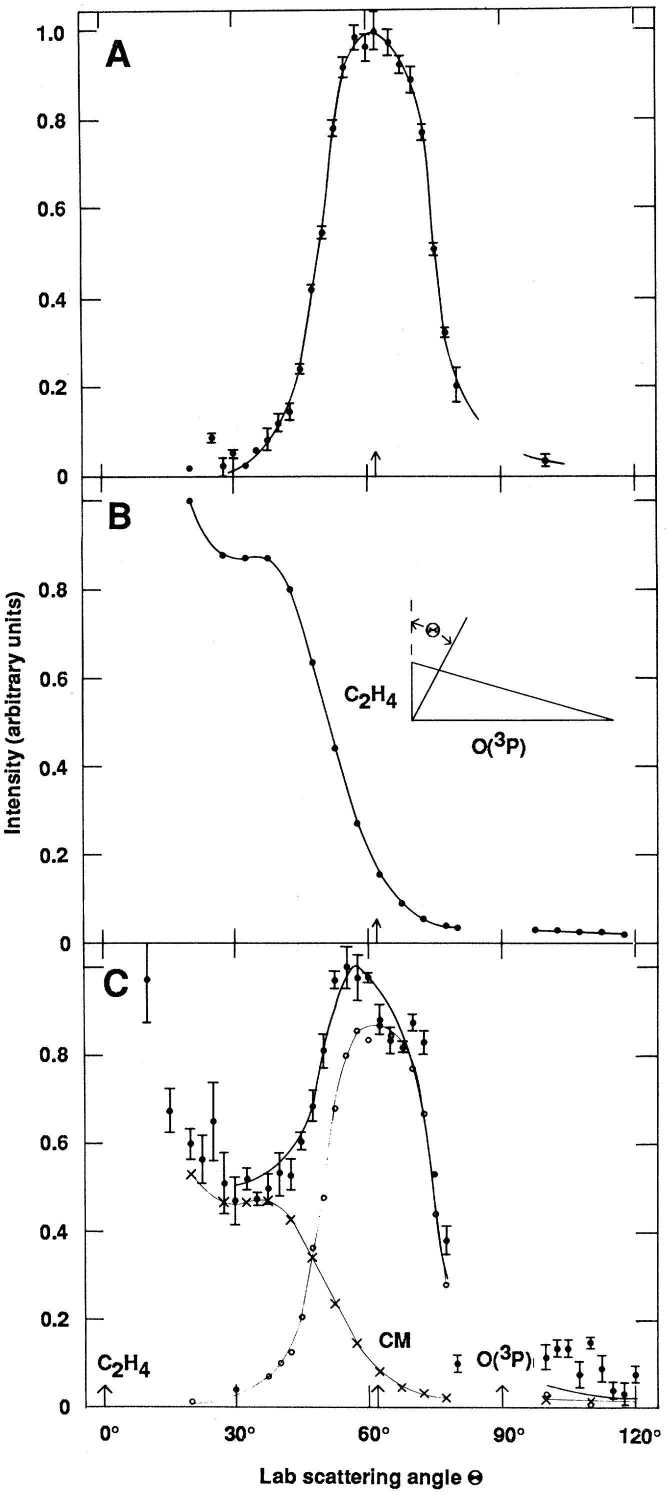

Fig. 7. Angular distributions from the reaction $O(^3P)$ + C_2H_4 at a collision energy of 10.7 kcal/ml. (**A**) CH_2CHO product; (**B**) elastic scattering of C_2H_4 monitored at *m/e* = 27 ($C_2H_3^+$); (**C**) *m/e* = 15 (CH_3^+); contributions from C_2H_4 and CH_2CHO are indicated by x and O, respectively. CM denotes the direction of the velocity vector of the center of mass of the entire system, measured from the direction of the beam of C_2H_4.

in the reaction intermediate and subsequent C–C rupture, as shown below, provides 90% of the products.

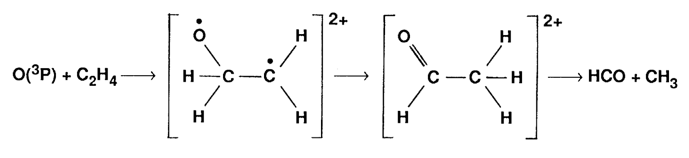

I

The remaining 10 percent is ketene formed by a three-center elimination of an H_2 molecule from the reaction intermediate.

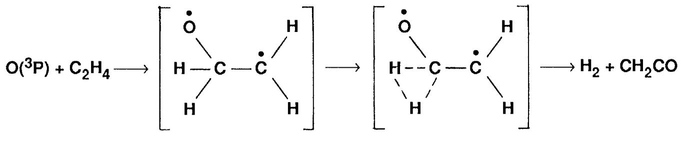

II

The measurements of product angular distributions in a crossed–molecular beam experiment (*30*), as shown in Fig. 7, gave strong evidence that the above conclusion was not quite correct. The fact that the intense $m/e = 42$ signal and the weak $m/e = 43$ signal (not shown) have the same angular distributions indicates that the substitution reaction forming vinyloxy radical, $CH_2CHO + H$, occurs. The $m/e = 42$ signal ($C_2H_2O^+$) results from dissociative ionization of CH_2CHO product rather than from the formation of CH_2CO and H_2. The formation of CH_2CO through the three-center elimination of a hydrogen molecule is expected to release a larger amount of recoil energy, and the fact that CH_2CO is recoiling from H_2 rather than from a hydrogen atom will cause the laboratory angular distribution of CH_2CO to be much broader than that of CH_2CHO. The $m/e = 15$ (CH_3^+) angular distribution clearly shows that in addition to reaction products, elastically scattered C_2H_4 molecules also produce CH_3^+ ions during ionization. The angular distribution of scattered C_2H_4 can be unambiguously measured at $m/e = 27$ ($C_2H_3^+$). After the contribution from elastically scattered C_2H_4 from the angular distribution at $m/e = 15$ has been subtracted, it is quite clear that the residual angular distribution of reactively scattered CH_3^+ has an identical angular distribution to that measured at $m/e = 43$ and 42. Apparently, most of the CH_3^+ from reactive scattering are also daughter ions of vinyloxy radicals, CH_2CHO. If the product channel $CH_3 + HCO$ were dominant, the angular distribution of CH_3^+ would be much broader. Without the measurement of product angular or velocity distributions, which reveal the parent-daughter relations, one would not have suspected that the simple substitution reaction forming vinyloxy radical

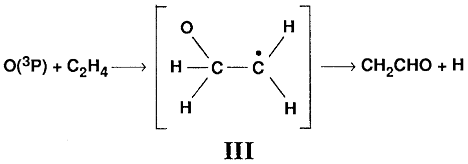

III

is in fact the major channel.

This was certainly a shocking discovery to chemical kineticists, since the reaction mechanism $O(^3P) + C_2H_4 \rightarrow CH_3 + HCO$ was thought to be well established. The important role played by the $CH_2CHO + H$ channel was never suspected. Several recent bulk studies using various time-resolved spectroscopic techniques (*31–35*) have verified the major role played by the hydrogen substitution channel indicated by the crossed–molecular beam experiments. These were not strictly single collision experiments, but all showed that the reaction channel $CH_2CHO + H$ accounted for at least half of the products.

Conclusion

The experimental investigation of elementary chemical reactions is presently in a very exciting period. The advance in modern microscopic experimental methods, especially crossed molecular beams and laser technology, has made it possible to explore the dynamics and mechanisms of important elementary chemical reactions in great detail. Through the continued accumulation of detailed and reliable knowledge about elementary reactions, we will be in a better position to understand, predict, and control many time-dependent macroscopic chemical processes that are important in nature or to human society.

In addition, because of recent improvements in the accuracy of theoretical predictions based on large-scale ab initio quantum mechanical calculations, meaningful comparisons between theoretical and experimental findings have become possible. In the remaining years of the 20th century, there is no doubt that the experimental investigation of the dynamics and mechanisms of elementary chemical reactions will play a very important role in bridging the gap between the basic laws of mechanics and the real world of chemistry.

REFERENCES AND NOTES

1. H. Eyring and M. Polanyi, *Z. Phys. Chem. Abt. B* **12**, 279 (1931).
2. J. C. Polanyi and D. C. Tardy, *J. Chem. Phys.* **51**, 5717 (1969).
3. J. H. Parker and G. C. Pimentel, *ibid.*, p. 91.
4. H. W. Cruse, P. J. Dagdigian, R. N. Zare, *Faraday Discuss. Chem. Soc.* **55**, 277 (1973).
5. D. P. Gerrity and J. J. Valentini, *J. Chem. Phys.* **82**, 1323 (1985).
6. D. R. Herschbach, in *Les Prix Nobel 1986* (Elsevier, Amsterdam, in press).
7. R. B. Bernstein, *Chemical Dynamics via Molecular Beam and Laser Techniques*, (Oxford Univ. Press, New York, 1982).
8. D. M. Neumark *et al.*, *J. Chem. Phys.* **82**, 3067 (1985).
9. Y. T. Lee, in *Atomic and Molecular Beam Method*, G. Scoles and U. Buck, Eds. (Oxford Univ. Press, New York, 1986).
10. Y. T. Lee, J. D. McDonald, P. R. LeBreton, D. R. Herschbach, *Rev. Sci. Instrum.* **40**, 1402 (1969).
11. J. T. Muckerman, in *Theoretical Chemistry—Advances and Perspectives*, H. Eyring and D. Henderson, Eds. (Academic Press, New York, 1981), vol. 6A, pp. 1–77.
12. C. F. Bender, P. K. Pearson, S. V. O'Neill, H. F. Schaefer, *J. Chem. Phys.* **56**, 4626 (1972); *Science* **176**, 1412 (1972).
13. D. G. Truhlar and A. Kuppermann, *J. Chem. Phys.* **52**, 384 (1970); *ibid.* **56**, 2232 (1972).
14. S.-F. Wu and R. D. Levine, *Mol. Phys.* **22**, 991 (1971).
15. G. C. Schatz, J. M. Bowman, A. Kupperman, *J. Chem. Phys.* **63**, 674 (1975).
16. A. Kuppermann, in *Potential Energy Surfaces and Dynamics Calculations*, D. G. Truhlar, Ed. (Plenum, New York, 1981), pp. 375–420.
17. J. M. Launay and M. LeDourneuf, *J. Phys. B* **15**, L455 (1982).
18. R. E. Wyatt, J. F. McNutt, M. J. Redmon, *Ber. Bunsenges. Phys. Chem.* **86**, 437 (1982).
19. D. M. Neumark, A. M. Wodtke, G. N. Robinson, C. C. Hayden, Y. T. Lee, *J. Chem. Phys.* **82**, 3045 (1985).
20. J. W. Birks, S. D. Gabelnick, H. S. Johnston, *J. Mol. Spectrosc.* **57**, 23 (1975).
21. J. M. Farrar, *J. Chem. Phys.* **63**, 3639 (1975).
22. M. J. Coggiola, J. J. Valentini, Y. T. Lee, *Int. J. Chem. Kinet.* **8**, 605 (1976).
23. C. C. Kahler and Y. T. Lee, *J. Chem. Phys.* **73**, 5122 (1980).
24. N. Abuaf, J. B. Anderson, R. P. Andres, J. B. Fenn, D. R. Miller, *Rarefied Gas Dynamics*, Fifth Symposium, C. L. Brundin, Ed. (Academic Press, New York, 1967), pp. 1317–1336.
25. G. N. Robinson, R. E. Continetti, Y. T. Lee, *Faraday Discuss. Chem. Soc.*, in press.
26. F. Huisken, D. Krajnovich, Z. Zhang, Y. R. Shen, Y. T. Lee, *J. Chem. Phys.* **78**, 3806 (1983).
27. R. J. Cvetanovic, *Can. J. Chem.* **33**, 1684 (1955).
28. F. J. Pruss, J. R. Slagle, D. Gutman, *J. Phys. Chem.* **78**, 663 (1974).
29. B. Blumenberg, K. Hoyerman, R. Sievert, in *Proceedings of the 16th International Symposium on Combustion* (Combustion Institute, Pittsburgh, 1977), p. 841.
30. R. J. Buss, R. J. Baseman, G. He, Y. T. Lee, *J. Photochem.* **17**, 389 (1981).
31. G. Inoue and H. Akimoto, *J. Chem. Phys.* **74**, 425 (1981).
32. H. E. Hunziker, H. Kneppe, H. R. Wendt, *J. Photochem.* **17**, 377 (1981).
33. F. Temps and H. G. Wagner, Bericht 18 Max Planck (Institut für Strömungotorschung, Göttingen, West Germany, 1982).
34. U. C. Sridharan and F. Kaufman, *Chem. Phys. Lett.* **102**, 45 (1983).
35. Y. Endo, S. Tsuchiya, C. Yamada, E. Hirota, *J. Chem. Phys.* **85**, 4446 (1986).
36. The experimental investigations described in this article would not have been possible without the dedicated efforts of my brilliant and enthusiastic co-workers during the past 20 years. I enjoyed working with them immensely and sharing the excitement of carrying out research together. Throughout these years, my scientific research activities have been supported by the Office of Basic Energy Sciences of the Department of Energy and the Office of Naval Research. The stable and continuing support and the confidence they have shown in my research have been most important and are gratefully appreciated.